NURETH14-111

EULERIAN SIMULATION OF INTERACTING PWR SPRAYS: INFLUENCE OF DROPLET COLLISIONS

A. Foissac¹, J. Malet¹, S. Mimouni², P. Ruyer¹, F. Feuillebois³ and O. Simonin⁴

¹ Institut de Radioprotection et de Sureté Nucléaire, Saclay, France

² Electricité de France, Chatou, France

³ Laboratoire d'Informatique pour la Mécanique et les Sciences de l'Ingénieur, Orsay, France

⁴ Institut de Mécanique des Fluides de Toulouse, Toulouse, France

Abstract

A numerical simulation of the interaction between two real Pressurized Water Reactor containment sprays is performed with a new model implemented into the Eulerian CFD code NEPTUNE_CFD. The water droplet polydispersion in size has been treated with a sectional approach. The influence of collisions between droplets is taken into account with a statistical approach based on the various outcomes of binary collision. Experiments were performed on a new facility, and data obtained are compared with this two-fluid simulation. The results show a good agreement.

Introduction

Spray systems are emergency devices designed for preserving the containment integrity in case of a severe accident in a Pressurized Water Reactor. These systems are used to prevent overpressure, to cool the containment atmosphere, to remove fission products from the containment atmosphere and to enhance the gas mixing in case of hydrogen presence in the reactor containment. The efficiency of these sprays can depend partially on the evolution of the droplet size distribution in the containment, due to gravity and drag forces, heat and mass transfers with the surrounding gas, and droplet collisions. Spray systems in nuclear power plants are composed of over 500 interacting water droplet sprays with droplet diameter range from $100~\mu m$ to $1000~\mu m$. They are used under pressure (2-3 bars) at temperature between $20^{\circ}C$ and $60^{\circ}C$, and under gaseous mixture composed of steam, hydrogen and air.

Droplet interactions are generally neglected in safety codes due to the lack of accurate industrial modelling of such sophisticated physics. However, studying droplet interactions in the field of spray systems in nuclear reactor containment is clearly justified, since more than 500 spray nozzles that are either oriented downwards or inclined are used in a PWR, resulting in an overlap of the spray envelops (Rabe et al. [1]).

The objective of this work is to present the model used for droplet collision numerical simulations and to compare the results with the experimental ones obtained on two interacting real PWR sprays.

1. PWR containment spray systems

The French PWR containments (Figure 1) have generally two series of nozzles placed in circular rows. More precisely, for the 900 MWe PWR, there are exactly four rings of nozzles having the characteristics presented in Table 1. A schematic view of these spray rings and the associated spray envelopes are given in Figure 1. The nozzle type used in many PWRs, in particularly French 900 MWe PWRs, is the so-called SPRACO 1713A, distributed by Lechler under reference 373.084.17.BN (Figure 1). This nozzle is generally used with water at a relative pressure of 350 kPa, producing a flow rate of approximately 1 l/s. The outlet orifice diameter is 9.5 mm. The temperature of the injected water during a hypothetical nuclear reactor accident is either from 20°C or 60°C to 100 °C, depending on the kind of process (the 60°C to 100°C process is the so-called recirculation mode).

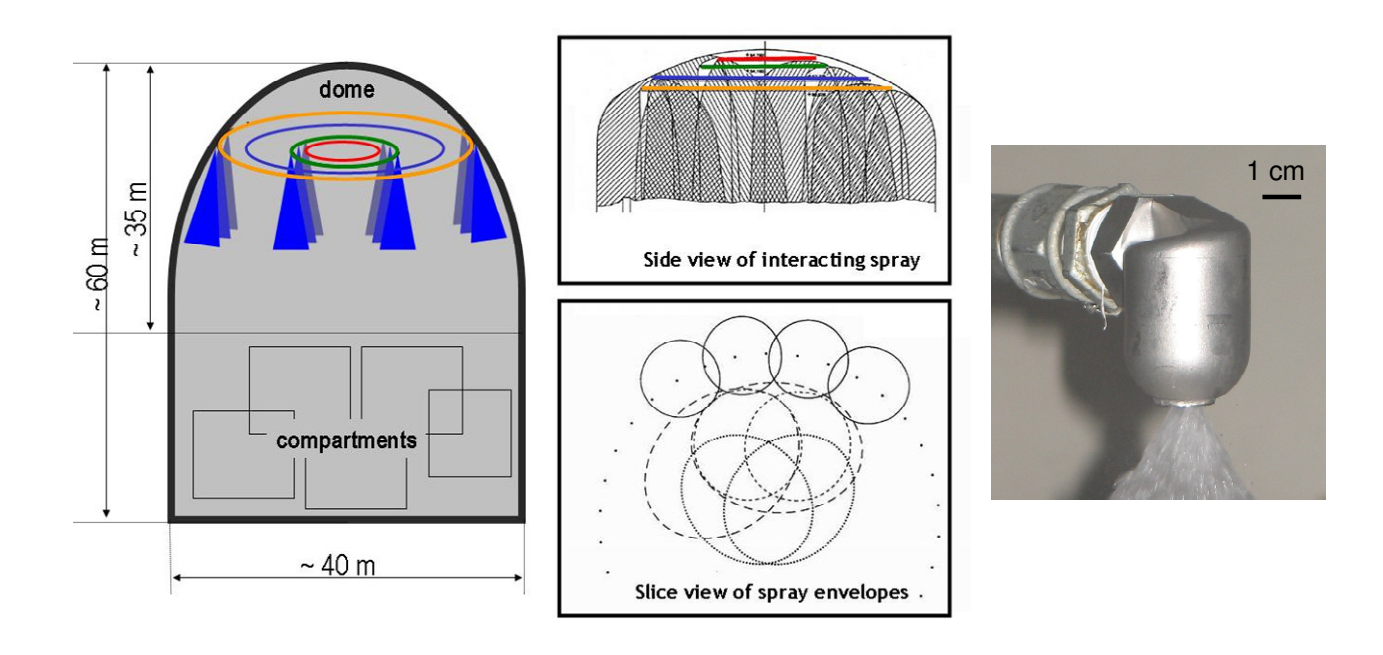


Figure 1 Spray rings and envelopes in a French PWR (not at scale) and spray nozzle SPRACO 1713A (Lechler 373.084.17.BN).

Table 1 Characteristics of spray rings for the French 900 MWe PWR.

	Height (m)	Diameter (m)	Number of nozzles	Approximated distance between nozzles (m)
1st Ring	54.8	10.0	66	0.5
2 nd Ring	54.2	14.8	68	0.7
3 rd Ring	52.3	22.5	186	0.4
4 th Ring	51.0	27.0	186	0.4

2. Experimental measurement of PWR containment spray characteristics

2.1 CALIST facility

Experiments have been carried out at the French Institute of Radiological Protection and Nuclear Safety (IRSN), on the CALIST facility (Characterization and Application of Large and Industrial Spray Transfer) sketched in Figure 2. In a room of 7 x 6 x 3.5 m³ dimensions, the set-up is composed of a supplying hydraulic circuit and, for these experiments, of two-interacting spray nozzles with a flow-rate of 1 l/s at a relative pressure of 350 kPa for each nozzle, and separated by 42 cm. The water spray, with a temperature of around 15 °C, is collected in a 5 m³ pool. The axial position of the spray nozzle may be changed using a monitored carriage.

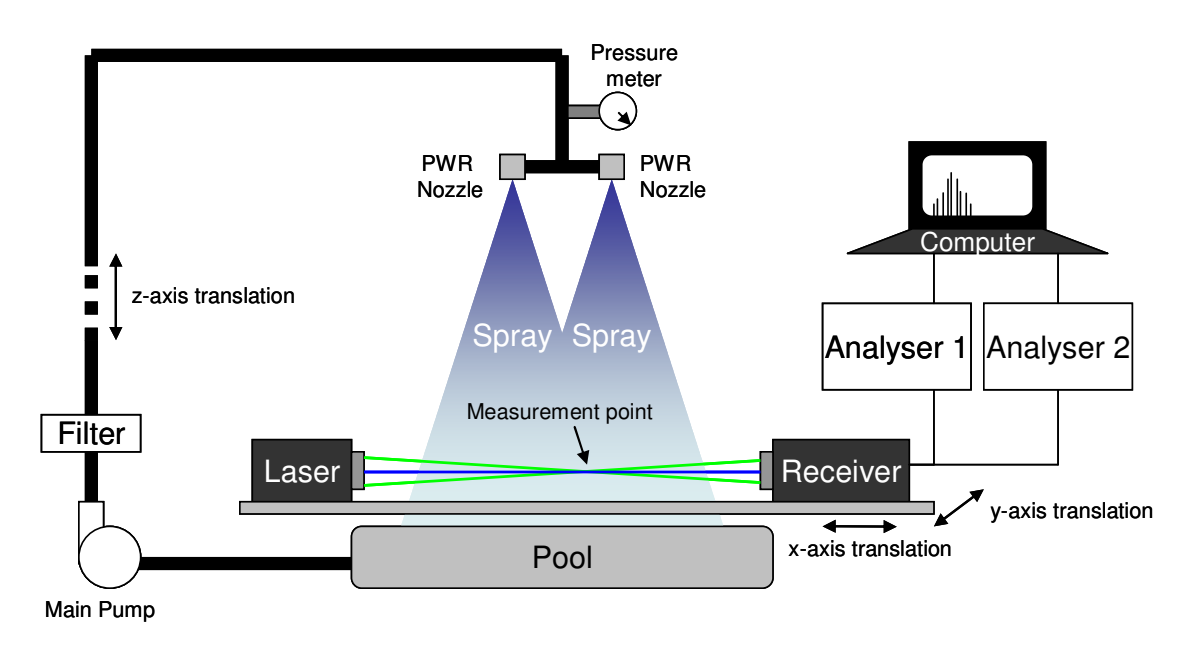


Figure 2 CALIST water-spray experimental facility.

The measurement of the spray characteristics requires a technique such as the light diffraction, shadowgraphy or Phase-Doppler Interferometry (PDI). The latter was chosen since it provides local high resolution information about the spray drops. Indeed, PDI measures the size and the velocity of drops passing through an optically defined probe volume (Bachalo and Houser [2]).

PDI can only measure droplets of spherical shape. In order to determine where atomization is achieved and so, when droplets are spherical, visualization has been performed with a Phantom high-speed camera used with a resolution of 800 x 600 pixels at a frequency of 4796 Hz, with an exposure time of 10 µs (Foissac et al. [3]). The spray is illuminated from the back in order to obtain consistent and machine readable images. The high-speed visualization shows that the distance from the nozzle exit at which most of the liquid is atomized into droplets is approximately 20 cm. Therefore, it can be anticipated that at such a distance, PDI measurements of droplets are reliable. Measurements have been performed at 20, 40, 50, 60, 80 and 100 cm from the nozzle exit. They have been performed three times for each position, and show a very good repeatability.

2.2 Characteristics of droplets at 20 cm from the nozzle

Measurements performed at 20 cm from the nozzles are used as inlet conditions of the numerical simulations. These nozzles are used at a relative pressure of 3.5 bar, for a mass flow rate of 1 kg/s. At this distance, due to the hollow cone created by these nozzles, most of the droplets are concentrated in an annular area located between 8 cm and 15 cm from the nozzle axis, with a maximum of presence at 11 cm. The geometric mean diameter (D_{10}), Sauter mean diameter (D_{32}) and mean velocities are displayed in Figure 3 as functions of the distance from the nozzle axis. D_{10} varies between approximately 240 μ m and 330 μ m. D_{32} varies between 360 μ m and 520 μ m. This implies dispersion in size. The axial velocity v_z is maximum close to the nozzle axis: it is 20 m/s at 8 cm, then decreases radially to 13 m/s at 15 cm. The radial velocity v_r is maximal far from the nozzle axis, and equals to 7.7 m/s. The orthogoadial velocity v_{θ} is very low, and varies between 0.17 m/s and 0.34 m/s. This means that the swirl created by the nozzle is attenuated very quickly in the first centimetres when atomization occurs. Figure 4 shows the local spray size and axial velocity distributions. It can be noticed that the shape of the size distribution does not depend on the distance from the nozzle axis. The size distribution can be approximated with a log-normal law [3]. The repeatability is very good for the D_{10} and axial velocity measurements. Uncertainties are higher for radial and orthoradial velocities, because direct measurements of these two values are not possible with our PDI.

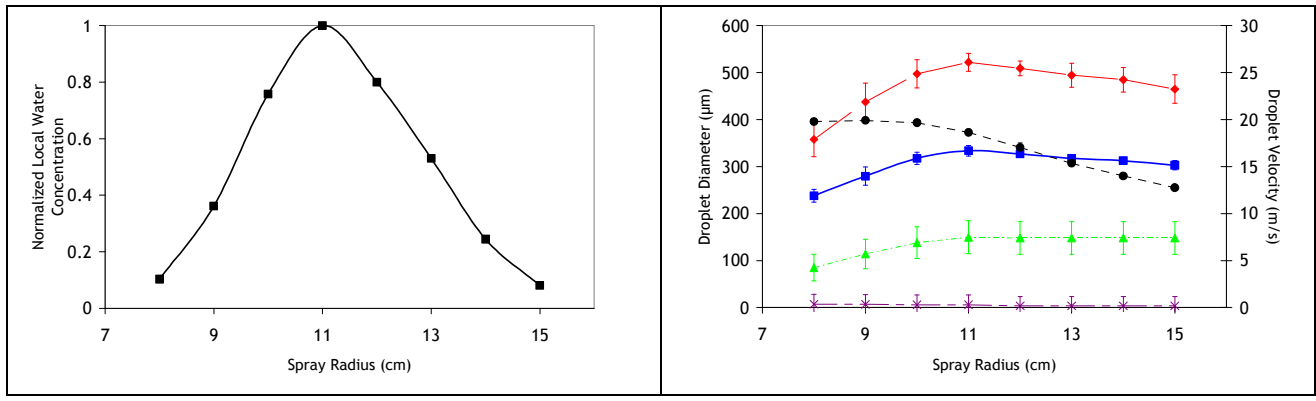


Figure 3 Mean characteristics of the spray at 20 cm from the nozzle outlet (error bars are given for an 67% interval of confidence).

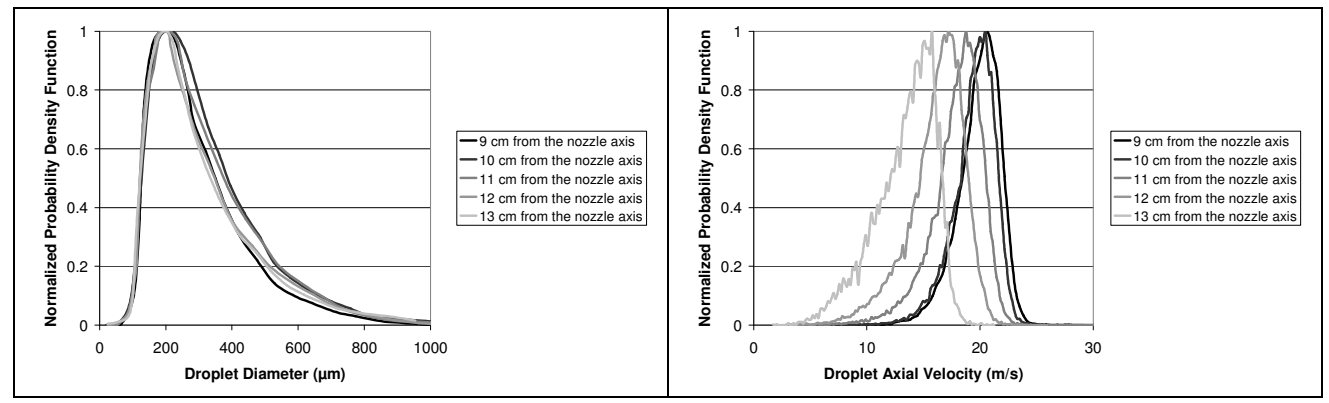


Figure 4 Experimental size and axial velocity distributions at 20 cm from the nozzle, presented for different distances from the nozzle axis.

Moreover, for each position, it is possible to give the size-velocity correlation. Indeed, each droplet size has its own mean velocity. These results are not presented in this paper but will be in a future one since they still need post-treatment of experimental data.

3. Modelling of droplet polydispersion and collisions

3.1 Modelling of droplet polydispersion

Greenberg et al. [4] developed a method to model particle polydispersion in size in Eulerian simulations. The idea was to consider the dispersed phase as a set of continuous "fluid" media: each "fluid" corresponding to a statistical average between two fixed droplet sizes, viz a section. The spray was then described by a set of conservation equations for each "fluid". In our case, both interacting sprays will be considered as independent fluids, and for each spray or fluid, size distributions are divided into sections of fixed diameter. Sections are chosen as fixed in size, and they exchange mass and momentum in order to model evaporation/condensation or collision phenomena.

3.2 **Modelling of droplet collisions**

The several-fluids model is constituted of a mass balance equation, where k represents each section, and i is the coordinate:

$$\frac{\partial}{\partial t} (\alpha_k \rho_k) + \frac{\partial}{\partial x_i} (\alpha_k \rho_k U_{k,i}) = \Gamma_k^{collision} + \Gamma_k^{cond/evap}$$
(1)

t is the time, α_k , ρ_k , $U_{k,i}$ denote the void fraction of section k, its averaged density and velocity along the coordinate i. $\Gamma_k^{collision}$ and $\Gamma_k^{cond/evap}$ are the mass transfer per unit volume and unit time due respectively to collisions and condensation/evaporation. It is assumed that no evaporation or condensation occurs in this case: $\Gamma_k^{cond/evap} = 0$.

 $\Gamma_k^{collision}$ is constituted of a source term Γ_k^{coll} and a sink term Γ_k^{coll} : $\Gamma_k^{collision} = \Gamma_k^{coll} + \Gamma_k^{coll}$

$$\Gamma_k^{collision} = \Gamma_k^{coll} + \Gamma_k^{coll} - \tag{2}$$

It can be written that:

$$\begin{cases}
\Gamma_k^{coll} + = \sum_{m,n} \Gamma_{m,n \to k} \\
\Gamma_k^{coll} - = -\sum_{m,n} \Gamma_{k,m \to n}
\end{cases}$$
(3)

Where $\Gamma_{m,n\to k}$ is the mass transfer from the section m to k after a collision between droplet of class m and droplet of class n.

The momentum balance equation is given by:

$$\frac{\partial}{\partial t} \left(\alpha_{k} \rho_{k} U_{k,i} \right) + \frac{\partial}{\partial x_{j}} \left(\alpha_{k} \rho_{k} U_{k,i} U_{k,j} \right) = -\alpha_{k} \nabla p + \alpha_{k} \rho_{k} g + \nabla \left[\alpha_{k} \left(\tau_{k} + \tau_{k}^{T} \right) \right] + \sum_{m,n} \Gamma_{m,n \to k} \left(U_{m,n \to k,i} - U_{k,i} \right)$$
(4)

p is the pressure, g the gravity. τ_k and τ_k^T denote the molecular and turbulent stress tensors (Reynolds stress tensor). $U_{m,n\to k,i}$ is the velocity of the section k along the coordinate i resulting from the collision between m and n.

 $\Gamma_k^{collision}$ and $\Gamma_{m,n\to k} \left(U_{m,n\to k,i} - U_{k,i} \right)$ can be calculated with a collision frequency and a modelling of collision issue. For this latter modelling, five binary collision regimes can be pointed out: bouncing, coalescence, reflexive separation, stretching separation and splashing (Roth et al. [5]). Looking at the collision pictures (Foissac et al. [6]), it is possible to determine the final daughter diameter as a function of the initial "parent" diameters, using mass conservation. These values are summarized in Table 2. For the splashing regime, a value of 20 droplets has been estimated, but it should be considered as a first approximation. All these collision issues can be represented by a graph depending on the Weber number and the impact parameter.

Table 2 Daughter droplets diameters of two parents droplets after a binary collision for different regimes.

Collision outcome	Small droplet diameter	Large droplet diameter	Final droplet diameter	Final direction velocity	Observations
Bouncing	d_s	d_{l}	d_s and d_l	v_s and v_l	No change
Coalescence			$\sqrt[3]{d_s^3 + d_l^3}$	$v_s + v_l$	Creation of one droplet
Stretching separation			d_s and d_l	v_s and v_l	Satellite droplets are neglected
Reflexive separation			$\sqrt[3]{\frac{d_s^3 + d_l^3}{3}}$	$v_s + v_l$	3 droplets are created
Splashing			$\sqrt[3]{\frac{d_s^3 + d_l^3}{20}}$	$v_s + v_l$	20 droplets are created

As shown in Rabe et al. [7], it is appropriate to define a symmetric Weber number starting from first mechanical principles. Using the momentum balance, and assuming that the droplets are spherical and have the same density, the symmetric Weber number is then expressed by:

$$We = \frac{\rho}{12\sigma} \frac{d_s^3 \|\vec{u}_s\|^2 + d_l^3 \|\vec{u}_l\|^2}{d_s^2 + d_l^2}$$
 (5)

Rabe et al. [7] proposed simple formulae expressing the boundaries of collision outcomes fields as a function of the symmetric Weber number. The final equation for the critical impact

parameter (I_c represents the impact parameter for which the transition between two regimes is observed) at which the transition between reflexive separation and coalescence occurs is then:

$$I_{c}^{ref-coal} = 3.59 \sqrt{1 - \frac{0.45}{We}}$$
 (6)

Based on another balance of energies, the critical impact parameter for the transition between coalescence and stretching separation can be expressed as:

$$I_{c}^{stre-coal} = \frac{\sqrt{We_{stre}^{2} + 8We_{stre}We} - We_{stre}}{4We} \quad \text{with } We_{stre} = 0.53$$
 (7)

For larger droplets and velocities, only separation regimes can be observed, namely reflexion and stretching. The ratio of the reflexive kinetic energy and the stretching kinetic energy can then be written and the critical impact parameter is then derived:

$$I_{c}^{ref-stre} = \sqrt{\frac{1-k}{1+R_{ref/stre}}}$$
 (8)

with k a viscous dissipation coefficient, found experimentally [7] to be equal to 0.92 and with dimensionless number $R_{ref/stre}$ that is found to be 0.25 according to experimental results [7].

These three models describing the transition curves between collision regimes are described in more details in Rabe et al. [7]. They are valid under ambient gas conditions for droplet sizes between 200 and 400 μ m, with velocities up to 10 m.s⁻¹.

Based on an energy balance, Estrade [8] proposed an equation for the transition to bouncing (where χ is the fraction of volume interaction and Δ the diameter ratio):

$$We_{coal/boun} = \frac{\Delta(1 + \Delta^2)(4\Phi_c - 12)}{\chi(1 - I^2)} \text{ with } \Phi_c = \frac{2}{\left(\frac{3}{\varphi_c^2} + 1\right)^{2/3}} + \left(\frac{3}{\varphi_c^2} + 1\right)^{1/3} \text{ and } \varphi_c = 0.458848 \quad (9)$$

Finally, splashing is assumed to occur when symmetrical Weber number is higher than 20 which is a very first modelling that needs to be confirmed by experiments.

It is also necessary to evaluate the collision frequency $f_{m,n}$ between droplets from sections m and n. Pigeonneau and Feuillebois [9] proposed the following expression:

$$f_{m,n} = g_0^{mn} \pi \left(\frac{d_m + d_n}{2} \right)^2 n_n n_m |U_m - U_n| \left[\left(\frac{1}{2z} + 1 \right) erf(\sqrt{z}) + \frac{\exp(-z)}{\sqrt{\pi z}} \right]$$
with $z = \frac{3}{4} \frac{(U_m - U_n)^2}{q_m^2 + q_n^2 - 2\sqrt{q_m^2 q_n^2}} \xi_m \xi_n$ (10)

Where d_m and d_n , n_m and n_n , q_m^2 and q_n^2 , and ξ_m and ξ_n are respectively the diameter, the number concentration, the droplet kinetic energy and the fluid-droplet velocity correlation coefficient of sections m and n. g_0 is the radial distribution function introduced by Patino and Simonin [10]:

$$g_0^{mn} = \left(1 - \frac{\sum_{p=m,n} \alpha_p}{0.64}\right)^{-0.64\gamma_{mn}} \text{ with } \gamma_{mn} = 1 + \frac{3}{2} \left(\frac{d_m d_n}{d_m + d_n}\right) \frac{2\sum_{p=m,n} \alpha_p / d_p}{\sum_{p=m,n} \alpha_p}$$
 (11)

Therefore, $\Gamma_k^{collision}$ and $\Gamma_{m,n\to k} (U_{m,n\to k,i} - U_{k,i})$ are obtained from the product of the collision frequency between sections m and n into the probability of a collision outcome derived from Rabe et al. [7], into the mass or velocity difference between the sections m and k associated to the collision outcome.

3.3 The NEPTUNE_CFD code

Numerical simulations have been performed using the NEPTUNE_CFD code (Mimouni et al. [11]). The solver belongs to the well-known class of pressure based methods. It is able to simulate multi-component multiphase flows by solving a set of three balance equations for each field (fluid component and/or phase). These fields can represent many kinds of multiphase flows: distinct physical components (e.g. gas, liquid and solid particles); thermodynamic phases of the same component (e.g.: liquid water and its vapour); distinct physical components, some of which split into different groups (e.g.: water and several groups of different diameter bubbles); different forms of the same physical components (e.g.: a continuous liquid field, a dispersed liquid field, a continuous vapour field, a dispersed vapour field). The solver is implemented in the NEPTUNE software environment, which is based on a finite volume discretization, together with a collocated arrangement for all variables. The data structure is totally face-based which allows the use of arbitrary shaped cells (tetrahedra, hexahedra, prisms, pyramids...) including no conforming meshes. The main interest of the numerical method is the so-called "volume fraction – pressure – energy cycle" that ensures mass and energy conservation and allows strong interface source term coupling. In the simulations described latter, gas turbulence is associated to the k-\varepsilon model, whereas dispersed phases turbulence is modelled with the Q2-Q12 model (Simonin [12]).

4. Numerical simulations of sprays

4.1 Validation of polydispersity and collision models on a simple case

Wunsch [13] performed Direct Numerical Simulations (DNS) of particle clouds in homogeneous isotropic turbulence, without gravity. Simulations were conducted with an initially log-normal distributed droplet phase, in a cubical domain with 128³ grid regular points for a physical length of cube of 0.128 m and with periodical boundary conditions. An overview of the physical properties is given in Table 3.

Table 3 Properties of fluid and initially log-normal distributed droplet phase [13]

Fluid density		Fluid kinematic viscosity			Fluid kinetic energy q_{fluid}^2	
1.17 kg/m ³		$1.47.10^{-5} \text{ m}^2/\text{s}$			$0.0015 \text{ m}^2/\text{s}^2$	
Droplet void fraction	Log-normal mean diameter		Log-normal standard deviation	Drop	olet density	$q_{ extit{droplet}}^2$ / $q_{ extit{fluid}}^2$
4.388 10 ⁻⁴	260 μ	m	0.12	220	5.3 kg/m ³	0.890

Figure 5 shows the size distribution evolution at different times, normalized on the initial distribution. It can be noticed that results from the sectional method described previously, used with 9 sections in the NEPTUNE_CFD code, are quite similar to the DNS ones. As a consequence, the sectional method and the polydispersity modelling are validated in the case of a homogeneous isotropic turbulence. Further numerical simulations should be performed to validate the drift part of the collision frequency (10), since this is the main phenomenon responsible for the collision in the top of the reactor containment.

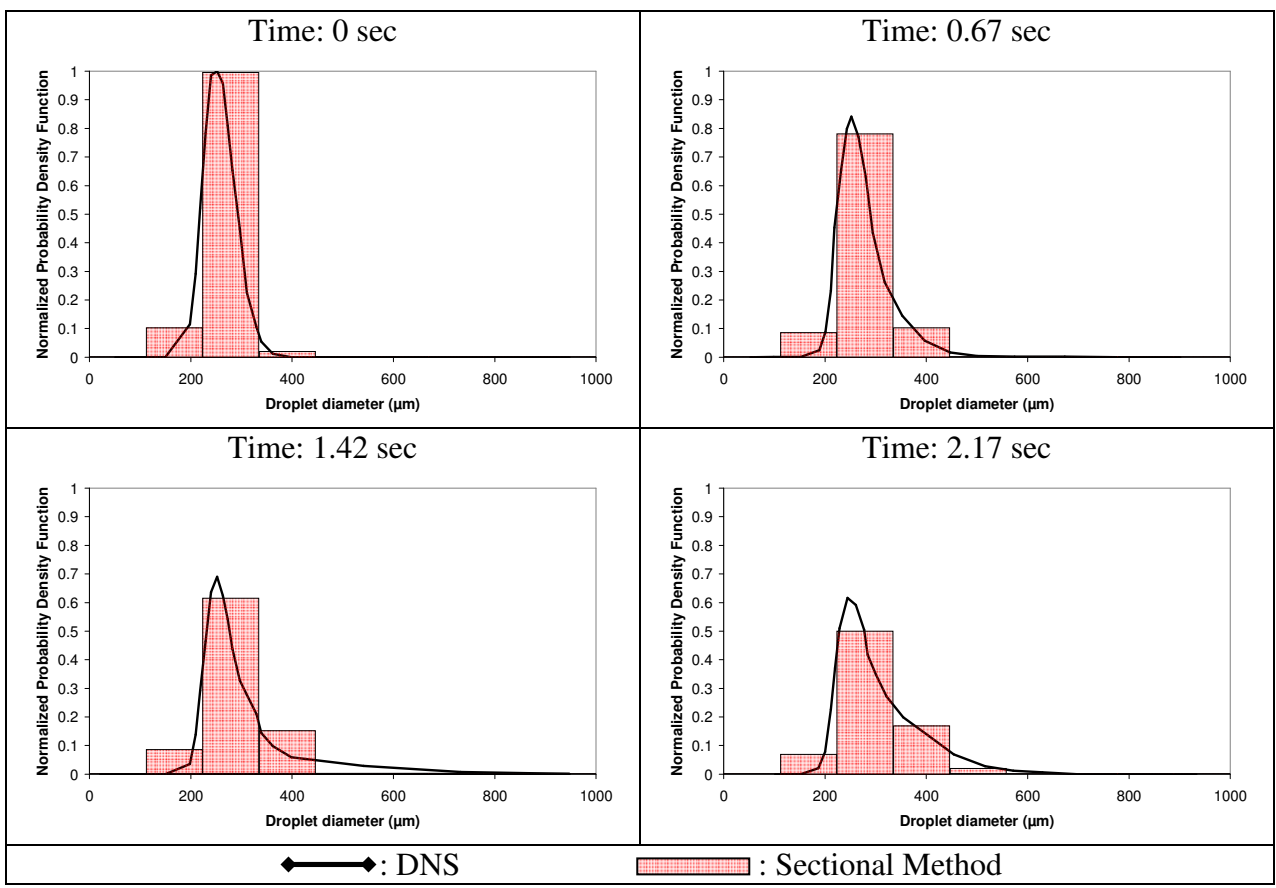


Figure 5 Droplet size distribution evolutions in time, comparison of DNS [13] and present sectional method.

4.2 Numerical simulation of two PWR interacting sprays

Interacting sprays, characterized on the CALIST facility, are simulated inside a parallelepiped mesh of 800,000 hexahedra regular cells, representing a domain of 1.20 x 0.80 x 2 m. All boundaries are considered as free outputs, except the top face which contains the input and walls around, with no friction, and where velocity can only be tangential. Since the spray produced by these nozzles is a hollow cone one to the location 20 cm from the nozzle, the input domain is modelled by two annular rings of 18 cm internal diameter and 26 cm external diameter. Droplets are injected from this annular ring with the size distribution presented in the Figure 4. On this figure, it can be seen that, in function of the distance to the nozzle axis, the axial velocity decreases from 20 m/s to 15 m/s.

In these simulations, it was assumed that the injection velocity is independent of the position; it was chosen with a value of 18.6 m/s, that is to say the velocity at 11 cm from the nozzle axis, where the volumetric fraction is maximal. Estimating the value of the radial velocity for the simulation is more difficult. Indeed, this value is very important since it is the main component of the relative velocity of the droplets when spray interacts, and so the value of the Weber number and the collision frequency. A value of 7.7 m/s was chosen according to the results presented in Figure 3. The orthoradial velocity was neglected due to its low value. Each spray size distribution was separated in 9 sections (Figure 6), whose void fractions were adjusted from the assumed droplet size distribution so as to obtain a mass flow rate of 1 kg/s, as measured on the real PWR nozzle for a relative pressure of 3.5 bar.

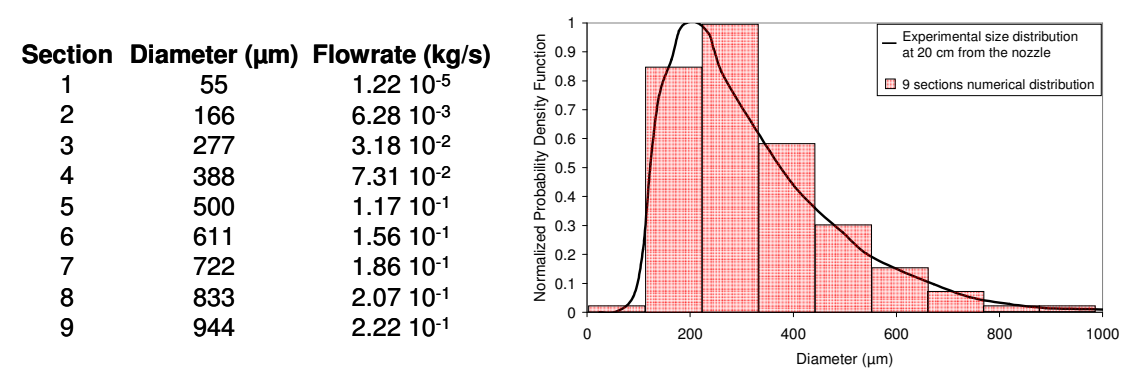


Figure 6 Sections used for the numerical simulation, associated to the experimental size distribution to the location 20 cm from the nozzle.

Experimental and numerical local size distributions obtained are compared in Figure 7 for different positions along the symmetrical axis. It is clear that the droplet size decreases since the mean geometric diameter is about 300 μm before spray interaction and about 200 μm after spray interaction (Figure 7). This decrease can have two origins. First, it can be due to collisions at high Weber number that occur when sprays interact: in the interaction area, collision frequency reaches a maximum of about 10¹¹ collisions.m⁻³.s⁻¹, and the Weber number is very high, so that collisions could lead to break up.

This size decrease is also due to the entrainment of the smallest droplets in the direction of the symmetrical axis (Cossali [14]). The smallest droplets are drifted away in the air flow, whereas the biggest droplets, having more inertia, are not altered in the spray interacting area. At this stage, we still have to separate the effects of these two phenomena.

Many parameters have to be tested in order to evaluate their influence. The first one is the radial velocity at the inlet, since it is involved in many critical parameters like the Weber number and the collision frequency. The difficulty is that its value is bound to an uncertainty in the measurement. The sensitivity to the mesh or the choice of intervals of the size distribution are also parts of the future work.

5. Conclusion

A numerical simulation of the interaction between two PWR containment sprays has been performed with a new model of polydispersion and collision of droplets, implemented into the

Eulerian CFD code NEPTUNE_CFD. The droplet size and velocity distributions at a distance of 20 cm below the spray nozzle outlet have been precisely measured and used as input data in the calculation. The water droplet polydispersion in size has been treated with a sectional approach. The influence of collisions between droplets is taken into account with a statistical approach based on the various outcomes of binary collisions. An elementary validation of one part of the collision model is performed, and our results are in good agreement with the DNS calculations. More elementary validations are needed, as for example a specific validation of the gas entrainment. An experiment of characterization of the gas entrainment by a single PWR spray will be performed on the CALIST facility. These results will allow to evaluate the ability of NEPTUNE_CFD code to simulate the gas entrainment produced with a spray where very few collisions occur.

A two-fluid multi-dimensional simulation, on the basis of two interacting real PWR spray nozzles, is compared to the results obtained on the CALIST facility and shows a good agreement. These first results allow us to continue on sensitivity studies in order to evaluate the most important phenomena involved in the droplet characteristics evolution (condensation, evaporation, entrainment, collision). The knowledge of these characteristics could be important to evaluate the efficiency of these spray systems in terms of depressurization, hydrogen mixing and radioactive aerosols scavenging for applications concerned by nuclear reactor accidents.

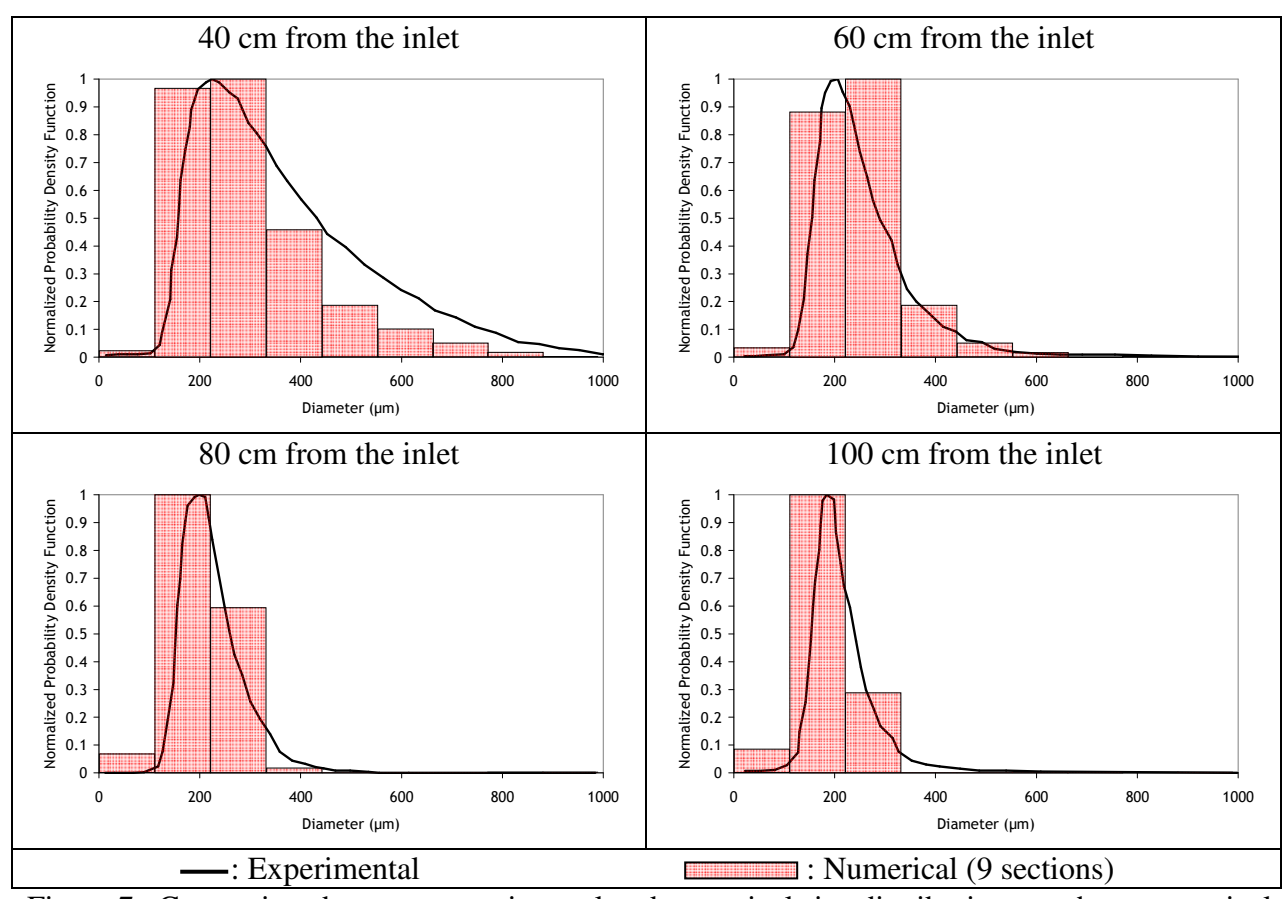


Figure 7 Comparison between experimental and numerical size distributions on the symmetrical axis and for different distances from the inlet.

6. References

- [1] C. Rabe, J. Malet and F. Feuillebois, "On the influence of droplet coalescence in spray systems for containment safety", *Proceedings of the 13th International Topical Meeting on Nuclear Reactor Thermal Hydraulics (NURETH-13)*, Kanazawa City, Japan, 2009.
- [2] W.D. Bachalo and M.J. Houser, "Phase Doppler spray analyzer for simultaneous measurements of drop size and velocity distributions", *Opt. Eng.*, Vol. 23, 1984, pp 583-590.
- [3] A. Foissac, J. Malet, R.M. Vetrano, J.M. Buchlin, S. Mimouni, F. Feuillebois and O. Simonin, "Experimental measurements of droplet size and velocity distributions at the outlet of a pressurized water reactor containment swirling spray nozzle", *Proceedings of XCFD4NRS-3*, Washington D.C., USA, 2010.
- [4] J.B. Greenberg, I. Silverman and Y. Tambour, "On the origin of spray sectional conservation equations", *Combustion and Flame*, Vol. 93, 1993, pp 90–96.
- [5] N. Roth, C. Rabe, B. Weigand, F. Feuillebois and J. Malet, "Droplet Collision Outcomes at HighWeber Number", *Proceedings of the 21st ILASS*, Mugla, Turkey, 2007
- [6] A. Foissac, J. Malet, S. Mimouni and F. Feuillebois, "Binary water droplet collision study in presence of solid aerosols in air", *Proceedings of the 7th ICMF*, Tampa, USA, 2010.
- [7] C. Rabe, J. Malet and F. Feuillebois, "Experimental investigation of water droplet binary collisions and description of outcomes with a symmetric Weber number", *Physics of fluids*, Vol. 22, 2010.
- [8] J.P. Estrade, "Experimental investigation of dynamic binary collision of ethanol droplets-a model for droplet coalescence and bouncing", *International Journal of Heat and Fluid Flow*, Vol. 20, 1999, pp 486-491.
- [9] F. Pigeonneau and F. Feuillebois, "Collision and size evolution of drops in homogeneous isotropic turbulence", *J. Aerosol Sci.*, Vol. 49, 1998, pp S1279-S1280.
- [10] G. Patino-Palacios and O. Simonin, "General derivation of eulerian-eulerian equations for multiphase flows", *Technical report*, IMFT, 2003.
- [11] S. Mimouni, J.-S. Lamy, J. Lavieville, S. Guieu, and M. Martin, "Modelling of sprays in containment applications with a CMFD code", *Nuclear Engineering and Design*, Vol. 240 (9), 2010, pp 2260–2270.
- [12] O. Simonin, "Combustion and turbulence in two-phase flows", von Karman Institute for Fluid Dynamics, Lecture Series, 1996-02, 1996.
- [13] D. Wunsch, "Theoretical and numerical study of collision and coalescence Statistical modeling approaches in gas-droplet turbulent flows", *PhD Thesis*, University of Toulouse, 2010.
- [14] G.E. Cossali, "An integral model for gas entrainment into full cone sprays", *J. Fluids Mechanics*, Vol. 439, 2001, pp 353-366.